

1 **Title:** Temperature-mediated changes in microbial carbon use efficiency and ^{13}C discrimination

2

3 **Author list and affiliations:**

4 C. A. Lehmeier¹, F. Ballantyne IV^{1,2}, K. Min¹, S. A. Billings^{1*}

5 ¹Department of Ecology and Evolutionary Biology, Kansas Biological Survey, University of
6 Kansas, 2101 Constant Ave., Lawrence, KS 66047, USA.

7 ²now: Odum School of Ecology, University of Georgia, 140 E. Green St., Athens, GA 30602,
8 USA.

9 ***Corresponding author:**

10 Sharon A. Billings, Kansas Biological Survey, University of Kansas, 2101 Constant Ave.,
11 Lawrence, KS 66047, USA. Tel.: 001-785-864-1560, Fax: 001-785-864-1534, email:
12 Sharon.Billings@ku.edu

13

14

15

16

17

18

19 **Abstract**

20 Understanding how carbon dioxide (CO₂) flux from ecosystems feeds back to climate warming
21 depends in part on our ability to quantify the efficiency with which microorganisms convert
22 organic carbon (C) into either biomass or CO₂. Quantifying ecosystem-level respiratory CO₂
23 losses often also requires assumptions about stable C isotope fractionations associated with the
24 microbial transformation of organic substrates. However, the diversity of organic substrates'
25 $\delta^{13}\text{C}$ and the challenges of measuring microbial C use efficiency (CUE) in their natural
26 environment fundamentally limit our ability to project ecosystem C budgets in a warming
27 climate. Here, we quantify the effect of temperature on C fluxes during metabolic
28 transformations of cellobiose, a common microbial substrate, by a cosmopolitan microorganism
29 growing at a constant rate. Specific respiration rate increased by 250% between 13 °C and 26.5
30 °C, decreasing CUE from 77% to 56%. Specific respiration rate was positively correlated with
31 an increase in respiratory ^{13}C discrimination from 4.4‰ to 6.7‰ across the same temperature
32 range. This first demonstration of a direct link between temperature, microbial CUE and
33 associated isotope fluxes provides a critical step towards understanding $\delta^{13}\text{C}$ of respired CO₂ at
34 multiple scales, and towards a framework for predicting future ecosystem C fluxes.

35

36 **1 Introduction**

37 Because Earth's C cycle is a key regulator of climate, a central goal of biogeochemistry is to
38 understand biosphere-atmosphere C exchange. Globally, almost all C initially assimilated via
39 photosynthesis is respired back to the atmosphere as CO₂ by auto- and heterotrophic organisms

40 (Schimel, 1995; Trumbore, 2006). Though we have a reasonably comprehensive understanding
41 of how environmental conditions influence CO₂ uptake by photosynthetic organisms, our
42 understanding of how respiratory CO₂ fluxes respond to environmental conditions significantly
43 lags behind. This is especially true for respiratory CO₂ derived from heterotrophs, which may
44 account for more than half of respiratory C losses from soils and aquatic systems (Kucera and
45 Kirkham, 1971; Hanson et al., 2000; Cotner and Biddanda, 2002; Subke et al., 2006). Metabolic
46 rates of heterotrophs are expected to increase with rising temperatures (Gillooly et al., 2001;
47 Pomeroy and Wiebe, 2001; Hall et al., 2008), which is of great concern given Earth's large
48 reservoir of reduced organic matter (OM) that may be mineralized to CO₂ via metabolism
49 (Hedges et al., 2000; Kirschbaum, 2006). The influence of temperature on the physiology of
50 heterotrophic microbes must therefore be well understood to project shifts in the global C
51 balance in a warmer climate.

52 Existing knowledge of Earth's terrestrial C balance has been bolstered by the use of stable
53 isotopes. A milestone for progress was when photosynthetic responses to environmental
54 conditions were linked to differences between the stable C isotopic composition ($\delta^{13}\text{C}$) of
55 atmospheric CO₂ and that of plant products (Farquhar et al., 1982). These differences, caused by
56 C isotope fractionation during CO₂ diffusion into leaves and subsequent carboxylation (Park and
57 Epstein, 1961; O'Leary, 1981), impart an isotopic fingerprint on ecosystem C pools and permit
58 inference about C fluxes from $\delta^{13}\text{C}$ of ecosystem C pools at multiple spatio-temporal scales
59 (Farquhar and Richards, 1984; Pataki et al., 2003; Dijkstra et al., 2004; Barbosa et al., 2010).
60 Recent studies remind us that respiratory C losses also leave an isotopic fingerprint on $\delta^{13}\text{C}$
61 values of plant tissues via respiration of substrates with distinct $\delta^{13}\text{C}$ (Bathellier et al., 2009;
62 Brüggemann et al. 2011; Ghashghaie and Badeck, 2014), and via C isotope fractionation during

63 decarboxylation in respiratory pathways (Werner and Gessler, 2011; Werner et al., 2011;
64 Tcherkez et al., 2012). Though not all C isotope fractionations during metabolism are well-
65 characterized, $\delta^{13}\text{C}$ of metabolic reaction substrates and products can vary predictably, caused by
66 kinetic or thermodynamic isotope effects (Rossmann et al., 1991; Gleixner and Schmidt, 1997;
67 Cleland, 2005; Tcherkez et al., 2012). Accounting for isotope effects in plant respiratory C
68 losses improves our ability to quantify the contributions of different pools to CO_2 fluxes and thus
69 our predictions of terrestrial ecosystem C budgets under changing environmental conditions.
70 Using $\delta^{13}\text{C}$ of heterotrophically respired CO_2 holds similar promise, but if and how changing
71 environmental conditions influence any fractionation factors for the fluxes associated with the
72 liberation of C from OM is unknown.

73 Significant uncertainty about the direction and magnitude of C isotope fractionation during
74 microbial C transformations (Bowling et al., 2008; Werth and Kuzyakov, 2010) renders
75 quantifying microbial CO_2 fluxes in ecosystems difficult. Difficulties arise because microbes in
76 natural systems can access a diverse array of organic substrates with distinct $\delta^{13}\text{C}$ signatures
77 (Park and Epstein, 1961; Billings, 2006), the respiration of which influences $\delta^{13}\text{C}$ of respired
78 CO_2 . Though we know the growth rate of microbial populations influences C flux into and
79 through biomass (Kayser et al., 2005), it is impossible to directly quantify microbial growth *in*
80 *situ*. Furthermore, absence of steady state conditions over a course of CO_2 flux measurements
81 makes the interpretation of temperature effects on the magnitude and the $\delta^{13}\text{C}$ of ecosystem
82 respiration an even greater challenge (Gamnitzer et al., 2011; Nickerson et al., 2013). Thus,
83 establishing a mechanistic understanding of the links between temperature, microbial respiration
84 rates and C isotope fractionation during substrate transformations at a fundamental level requires

85 that we characterize these processes as temperature changes in isolation from other factors that
86 influence microbial C transformations.

87 To assess the influence of temperature on microbial growth and respiration rates, we grew a
88 widely distributed Gram-negative, heterotrophic bacterium (*Pseudomonas fluorescens*) in
89 continuous culture bioreactors (chemostats) at seven temperatures ranging from 13 °C to 26 °C
90 (Fig. 1) at reactor dilution rates of approximately 0.14 h⁻¹, which is equivalent to the relative
91 growth rates of the microbial populations (Dawson, 1974; Smith and Waltman, 1995; Goldman
92 and Dennett, 2000; Chrzanowski and Grover, 2008; Ferenci, 2008; Bull, 2010; Egli, 2015). We
93 measured microbial respiration rates and $\delta^{13}\text{C}$ of respired CO₂ in this open, flow-through system
94 at steady-state (Craig and Gordon, 1965; Fry, 2006; see Supplementary Material for a detailed
95 elaboration of this approach). We computed the temperature dependence of a widely applied
96 metric of microbial C use efficiency (CUE), defined as SGR / (SGR+SRR), where SGR and SRR
97 are specific growth and specific respiration rates respectively, with units of C per microbial
98 biomass-C and time. Our simplified system eliminates factors present in natural environments
99 that preclude accurate assessment of specific growth and respiration rates, and thus accurate
100 estimates of CUE as defined above. Obtaining accurate estimates of microbial CUE is critical
101 for projecting C fluxes into the future because the particular value of CUE significantly
102 influences CO₂ loss rates from ecosystems in models of OM decomposition (Allison et al., 2010;
103 Wieder et al., 2013). Finally, simultaneously quantifying differences in $\delta^{13}\text{C}$ of organic substrate,
104 microbial biomass and respired CO₂ along a temperature gradient is critical for partitioning
105 synoptic CO₂ measurements into component fluxes.

106

107 **2 Materials and Methods**

108 **2.1 Pre-cultivation of microorganisms for chemostat inoculation**

109 We pre-cultivated *Pseudomonas fluorescens* (Carolina Biological Supply, USA) in nutrient
110 solution containing 10 mM NH₄Cl, 1.6 mM KNO₃, 2.6 mM K₂HPO₄, 1.0 mM KH₂PO₄, 0.8 mM
111 MgSO₄, 0.2 mM CaCl₂, 0.1 mM CuCl₂, 0.04 mM FeSO₄, 0.03 mM MnCl₂ and 0.02 mM ZnSO₄,
112 modified from Abraham et al. (1998). The sole C source in the nutrient medium was 10 mM
113 cellobiose (C₁₂H₂₂O₁₁; with a $\delta^{13}\text{C}$ of -24.2‰); cellobiose is a disaccharide consisting of two
114 glucose molecules and a basic module of cellulose. Thus, the C to N to P atomic ratio of the
115 autoclaved, sterile nutrient solution was 100 to 10 to 3.3; its pH was adjusted to 6.5. The
116 bacteria grew for a few days in batch culture in a flask fitted with a vent for air exchange covered
117 by a 0.22 μm filter (Fisher Scientific, USA) to avoid contamination. Vessel contents were stirred
118 continuously in an incubator maintained at 10 °C.

119 **2.2 The laboratory mesocosm – the chemostat**

120 The chemostat system was composed of two 1.9 L vessels, a medium reservoir tank and a
121 reactor, each maintained on separate heating/stirring plates (Fig. 1) in separate incubators. The
122 reactor volume was on average 870 mL (Supplementary Table 1). The reservoir tank was
123 connected via a flexible tube to the reactor (Tygon E-LFL pump tubing, Masterflex, USA),
124 which in turn had an outlet tube (Fig. 1; both tubes had a 1.6 mm inner diameter). When the
125 chemostat was operated in “continuous culture mode” a peristaltic pump transported fresh
126 medium to the reactor and simultaneously removed medium from the reactor at the same rate.
127 Thus, reactor volume remained constant during all chemostat runs. The 0.22 μm filter in the

128 reservoir tank lid allowed for pressure compensation during withdrawal of nutrient solution in
129 the continuous flow mode. Experimental temperatures were continuously measured with a
130 thermometer (Oakton, USA) placed in the reactor medium (Fig. 1). This thermometer was
131 routinely compared against an internal laboratory standard mercury thermometer, before and at
132 the end of each experiment. The reactor temperatures were adjusted with heating/stirring plate
133 and incubator settings, and kept constant during all experimental runs.

134 The reactor lid had two ports for gas lines. The outlet port tube was connected to a $^{13}\text{CO}_2/^{12}\text{CO}_2$
135 analyzer (G2101-i, Picarro, USA) containing a pump that continuously removed air from the
136 reactor headspace at an average rate of 0.025 L min^{-1} . A water trap (magnesium perchlorate,
137 Costech, USA) was installed between outlet port of the reactor and the gas analyzer. The CO_2
138 analyzer recorded the concentration and the $\delta^{13}\text{C}$ of the reactor headspace CO_2 at 0.5 Hz. The
139 reactor's inlet tube was connected to a mass flow controller (MC-50SCCM, Alicat Scientific,
140 USA), which in turn, was connected to a gas cylinder containing CO_2 -free air (Fig. 1). The mass
141 flow controller was programmed to maintain the reactor headspace at constant atmospheric
142 pressure; thus, the 0.025 L min^{-1} headspace air removed by the $^{13}\text{CO}_2/^{12}\text{CO}_2$ analyzer pump was
143 instantaneously replaced with CO_2 -free air flowing from the gas cylinder into the reactor
144 medium. Assuming (1) that 1 mol of O_2 is consumed per 1 mol of CO_2 produced in aerobic
145 respiration, (2) a typical reactor headspace CO_2 concentration of around 2000 ppm at steady state
146 (see Fig. 2A and below), and (3) an O_2 concentration of 21% in the air supply to the reactor, the
147 air supply permitted continuous aerobic metabolism. Routine tests with CO_2 -free air in sterile
148 chemostats were performed to ensure there were no leaks in the system.

149 **2.3. The chemostat run – standardized protocol and description of events**

150 We conducted seven independent chemostat runs, at temperatures of 13, 14.5, 16, 18, 21, 23.5
151 and 26.5 °C, in random temporal order. For each of the chemostat runs, we inoculated the
152 reactor with a 10 mL aliquot of the *P. fluorescens* pre-culture and activated the flow of CO₂-free
153 air through the reactor; this was considered time 0. At the initial stage of a chemostat run, the
154 bacteria grew in batch culture, that is, there was no flow of fresh nutrient medium from the
155 reservoir tank to the reactor, and no removal of medium from the reactor (Fig. 1).

156 **2.3.1 Respiration measurements at chemical and isotopic equilibrium in the continuous
157 flow chemostat at steady-state**

158 At the initial pH of 6.5, inorganic C in the fresh reactor medium was mainly in the form of
159 H₂CO₃ (aq) and HCO₃⁻ (Stumm and Morgan, 1981). By continuously bubbling CO₂-free air into
160 the reactor, we expelled these initial inorganic C pools from the reactor medium. This was
161 evident by concentrations of reactor headspace CO₂ of virtually zero in the early stages of batch
162 culture after each run's inoculation (Fig. 2A). During the phase of rising reactor headspace CO₂
163 via respiratory activity of the exponentially growing population (Fig. 2A), inorganic C in the
164 reactor medium accrued with the increasing addition of CO₂ from microbial respiration. That is,
165 at any point in time during the phase of increasing reactor headspace CO₂ concentration, the
166 nutrient medium acted as a sink for respired CO₂ (see also Supplementary Material).

167 Once the respiratory activity of the growing microbial population pushed the reactor headspace
168 CO₂ concentration above 500 ppm, we transferred the chemostat into the “continuous culture,
169 open system” mode (Figs. 1, 2; Ferenci, 2008; Bull, 2010). The peristaltic pump henceforth
170 transported fresh nutrient medium from the reservoir tank to the reactor at a constant rate of, on
171 average, 118 mL h⁻¹ (Supplementary Table 1), and simultaneously removed medium from the

172 reactor at the same rate so that the reactor volume remained constant. Initial chemostat
173 experiments indicated that when headspace CO₂ concentrations reached 500 ppm, the bacterial
174 population was sufficiently dense to maintain itself without being washed out via dilution.
175 Depending on the reactor temperature, the onset of the continuous culture mode occurred
176 between 40 h (at 26.5 °C) and 72 h (at 13 °C) after inoculation.

177 After the switch from batch to continuous culture, the rate of increase in reactor headspace CO₂
178 concentration gradually slowed because cells were continuously diluted into the waste stream
179 (Fig. 1), and approached a phase where the CO₂ concentration became stable (Fig. 2A). At this
180 point, bacteria grown in continuous culture had reached the phase of steady-state growth and
181 physiology (see Ferenci, 2008; Bull, 2010). A key feature of the continuous culture chemostat
182 relevant to our study is that at this steady-state, the constant dilution rate of the reactor (the
183 medium flow rate divided by the reactor volume) is equivalent to the specific growth rate of the
184 microbial culture (Bull, 2010). That is, washout of cells with the nutrient medium flow is
185 balanced by cell division so that the size of the population in the reactor can be expected to be
186 reasonably constant in the time frames employed here (see discussion in Ferenci, 2008; Bull,
187 2010).

188 Critically, when reactor headspace CO₂ concentrations approached the steady-state, inorganic C
189 pools came to their respective equilibria as well (Stumm and Morgan, 1981). At this point, pools
190 of H₂CO₃ (aq) and HCO₃⁻ were no longer a *net* sink for respired CO₂. As reactor headspace CO₂
191 concentrations reached steady state, the system supported constant microbial CO₂ production
192 reflective of steady-state growth under constant environmental conditions, and reflected
193 chemical equilibrium (i.e., constant size) of the dissolved inorganic C pools. Thus, the rate of

194 CO₂ addition to the reactor headspace volume at steady-state accurately represented the CO₂
195 released during microbial respiration (see also Supplementary Material).

196 We calculated the molar CO₂ production rate of the microbial population as the product of the
197 average molar CO₂ concentration measured by the ¹³CO₂/¹²CO₂ analyzer for 5 hours at steady
198 state (Fig. 2A) multiplied by the molar air flow rate through the reactor, which was calculated as

199 Air flow (mol min⁻¹) = 0.96 atm * 0.025 L min⁻¹ / (0.082 atm L mol⁻¹ K⁻¹ * 296 K),

200 with 0.96 atm and 296 K being the barometric pressure and the temperature in the lab where the
201 experiments were performed, 0.025 L min⁻¹ the average volumetric headspace flow rate through
202 the reactor and 0.082 atm L mol⁻¹ K⁻¹ the gas constant.

203 The $\delta^{13}\text{C}$ of the reactor headspace CO₂ during the earliest batch culture phase was generally very
204 negative; the ¹³CO₂/¹²CO₂ analyzer cannot accurately measure ¹³C and ¹²C in very low CO₂
205 concentrations (Fig. 2B). The $\delta^{13}\text{C}$ of reactor headspace CO₂ became less negative as the CO₂
206 concentration increased (Fig. 2B). During the “climbing” phase of the reactor headspace CO₂,
207 the $\delta^{13}\text{C}$ of the CO₂ pool was influenced by isotopic fractionation among gaseous CO₂, H₂CO₃
208 (aq) and HCO₃⁻ (Vogel et al., 1970; Mook et al., 1974; Stumm and Morgan, 1981; Szaran, 1997),
209 because the dissolved inorganic C pools functioned as a net sink for respired CO₂. At steady-
210 state, with constant headspace CO₂ concentrations and constant size of the dissolved inorganic C
211 pools (see above), isotopic equilibrium was achieved, evidenced by constant $\delta^{13}\text{C}$ readings of
212 reactor headspace CO₂ (Fig. 2B). As such, in this open system at steady-state, the $\delta^{13}\text{C}$ of the
213 CO₂ leaving the reactor (the CO₂ measured by the analyzer) is identical to the $\delta^{13}\text{C}$ of microbial
214 respiration (Craig and Gordon, 1965; Fry, 2006). Importantly, this principle is valid irrespective

215 of temperature, microbial growth rate or microbial biomass in the reactor. (See Supplementary
216 Material for an elaboration of the principle of chemical and isotopic equilibrium.)

217 We used the average $\delta^{13}\text{C}$ measurement of reactor headspace CO_2 over the same five hours in the
218 stable phase employed for calculations of microbial respiration rates (see above) as the isotopic
219 signature of CO_2 respired by the microbial culture at each temperature. Any measurements of
220 headspace CO_2 and $\delta^{13}\text{C}$ during the climbing phase before steady-state (Fig. 2) were not used in
221 these calculations.

222 For the example chemostat at 23.5 °C, the half-life of the reactor ($t_{1/2}$), i.e., the time it took until
223 50% of the reactor medium was exchanged with fresh tank medium, was 5.2 h (with $t_{1/2} = \ln(2) /$
224 (medium flow rate / reactor volume); Supplementary Table 1). In a homogeneous, well-mixed
225 system such as that employed here, 95% of the pool (i.e., the reactor) is exchanged with new
226 medium within approximately five times the half-life. Thus, during the respiration
227 measurements between time 70 h and 74 h (in the example time course in Fig. 2), any “leftovers”
228 from the batch culture mode were insignificant, and the microbial culture could be considered
229 homogeneous. This principle was applicable to all chemostat runs we performed.

230 After the 5-hour respiration measurements were completed, we disconnected the gas lines from
231 the reactor, connected the mass flow controller directly to the $^{13}\text{CO}_2/^{12}\text{CO}_2$ analyzer, and replaced
232 the CO_2 -free air cylinder with a reference gas cylinder containing 1015 ppm CO_2 at a $\delta^{13}\text{C}$ of -
233 48.9‰ (Matheson, USA). This laboratory standard gas was previously calibrated against
234 secondary CO_2 standards (Oztech, USA) and served for any necessary corrections of the $\delta^{13}\text{C}$ of
235 the reactor headspace CO_2 measurements. Across the seven standard measurement procedures
236 after each individual chemostat run, the $\delta^{13}\text{C}$ measured for the laboratory standard gas showed

237 only slight variation (1 SD = 0.16%). CO₂ concentration measurements needed no correction;
238 measurements of lab-internal gases with previously determined CO₂ concentrations between
239 chemostat runs showed very stable and accurate analyzer performance.

240 **2.3.2 Measurements of extracellular enzyme activities at steady-state**

241 Using principles detailed by Lehmeier et al. (2013) and Min et al. (2014), we tested reactor
242 medium for activity of the extracellular enzymes β -glucosidase and β -N-acetyl glucosaminidase
243 across all chemostat temperatures; we never detected extracellular activity of either enzyme. The
244 lack of extracellular β -glucosidase activity indicates that the sole C source, cellobiose, was
245 directly taken up by microbes and cleaved intracellularly into glucose monomers for further
246 metabolism. The lack of extracellular β -N-acetyl glucosaminidase activity suggests that the
247 inorganic N provided in nutrient medium was the sole source of N taken up by *P. fluorescens*.
248 These findings do not rule out the possibility that *P. fluorescens* may have taken up (i.e. recycled)
249 any exuded C-based metabolic compounds, although such a scenario in continuous culture
250 conditions may not appear to be energetically favorable. Thus, the assumption that the sole
251 resources used by *P. fluorescens* were the cellobiose and the nutrient medium appears reasonable.

252 **2.3.3 Harvest of microbial biomass at steady-state**

253 Immediately after completing the 5 hour respiration measurements, we filtered approximately
254 300 mL of reactor medium for steady-state microbial biomass using 0.2 μ m filters made of
255 polyethersulfone (Pall, USA) and a vacuum pump. The filters had previously been oven-dried
256 for 48 h at 75 °C and their dry weight determined. We then oven-dried the filters post filtration
257 for 48 h at 75 °C, removed some of the dry biomass and weighed 1.2 mg of the material into tin

258 cups for subsequent combustion in an elemental analyzer (1110 CHN Combustion Analyzer,
259 Carlo Erba Strumentazione, Italy) coupled to a ThermoFinnigan DeltaPlus mass spectrometer
260 (Finnigan MAT, Germany) at the Keck Paleoenvironmental and Environmental Stable Isotope
261 Laboratory (The University of Kansas, USA). We thus determined biomass C (and N) elemental
262 content, as well as the $\delta^{13}\text{C}$ of the biomass. In this analysis, the samples were compared against
263 a laboratory standard CO_2 previously calibrated against the same secondary CO_2 standards as
264 used in calibration of the CO_2 standard used for respiration measurements (see above). The $\delta^{13}\text{C}$
265 of the substrate cellobiose was measured likewise. Dry weight of the sampled reactor aliquots
266 and the C content obtained from elemental analysis served to calculate total microbial C content
267 in the steady-state reactor and to calculate specific respiration rates.

268 At all temperatures studied, biomass C and N contents were virtually the same, on average 27%
269 and 8% of microbial dry mass, respectively (Supplementary Table 1). From mass balance
270 calculations, we determined that only a small percentage of the C and N supplied via fresh
271 medium from the tank was taken up to fuel microbial growth (2.8 % and 4.3 % on average for C
272 and N, respectively). This suggests that the observed temperature effects on specific respiration
273 rates and CUE were not confounded by any differences in C and N limitations at the different
274 temperatures (Goldmann and Dennet, 2000; Cotner et al., 2006; Chrzanowski and Grover, 2008).

275

276 **3 Results and Discussion**

277 For *P. fluorescens* grown in continuous culture, CUE, defined as SGR / (SGR + SRR), declined
278 with increasing temperature, from 77% at 13 °C to 56% at 26.5 °C (Fig. 3A). Because specific

279 growth rates were similar across the experimental temperatures (137 mg g⁻¹ h⁻¹, \pm 8 (1 SD); or
280 13.7 % h⁻¹ in relative terms; Fig. 3B), the decline in CUE was due to the 2.5 fold increase of SRR
281 with temperature, which rose from 45 mg g⁻¹ h⁻¹ at 13 °C to 113 mg g⁻¹ h⁻¹ at 26.5 °C (Fig. 3B).
282 The decline in CUE is also evident in the more than 50% reduction in steady-state dry microbial
283 biomass with increasing temperature (Fig. 3A). For example, though SGR was approximately
284 the same and thus the fraction of biomass replaced per time similar across all experimental
285 temperatures (0.147 and 0.141 at 13 °C and 26.5 °C, respectively; Fig. 3B) microbes at 13 °C
286 generated 20.9 mg biomass h⁻¹ while those at 26.5 °C generated less than half the amount (9.5
287 mg biomass h⁻¹).

288 Because we did not quantify possible C losses from the population at steady-state such as
289 secretion of organic acids or other compounds (El-Mansi and Holms, 1989; Nanchen et al.,
290 2006), gross rates of steady-state cellobiose C uptake may have been slightly higher than what
291 was calculated from the sum of SGR and SRR. However, the direct observation of *P.*
292 *fluorescens*' CUE is consistent with the negative effect of increasing temperature on microbial
293 CUE widely reported in literature for soils and aquatic ecosystems (del Giorgio and Cole, 1998;
294 Gillooly et al., 2001; Rivkin and Legendre, 2001; Apple et al., 2006; Manzoni et al., 2012; Frey
295 et al., 2013; Tucker et al., 2013).

296 Across the chemostat runs, we observed strong C isotope fractionations, which created
297 pronounced differences in $\delta^{13}\text{C}$ between microbial biomass and the sole C substrate, cellobiose,
298 and between microbial biomass and respired CO₂ (Fig. 4). Microbial biomass exhibited 5.5 to
299 10.5‰ more negative $\delta^{13}\text{C}$ values than the cellobiose and respired CO₂ was even more ^{13}C
300 depleted, at least 4.4‰ more negative than the biomass (Fig. 4A). Because each chemostat was

301 at steady-state, isotopic mass balance dictates that ^{13}C “missing” from cellobiose had to
302 accumulate in another pool in the reactor. The only pool that could have been enriched with the
303 “missing” ^{13}C was reactor DOC, which we analyzed for $\delta^{13}\text{C}$ in four out of the seven chemostat
304 runs (Fig. 4A). Reactor DOC consisted of a large pool of cellobiose (because the rate of C
305 consumption by the chemostat cultures was, on average, only 2.8% of the rate of C supply) and
306 presumably a pool of additional organic compounds (e.g. acetate). Such compounds appear to be
307 typically secreted from microbial cells at low rates in aerobic chemostats operated at dilution
308 rates similar to those of our runs (El-Mansi and Holms, 1989; Nanchen et al., 2006), and have
309 been shown to be enriched in ^{13}C compared to cellular biomass (Blair et al., 1985). However,
310 because such a small fraction of the available cellobiose was taken up by *P. fluorescens*, the
311 fraction of total DOC comprised of secreted organic compounds was small. As a result, ^{13}C
312 enrichment of any microbial exudates was insufficient to enrich bulk DOC to an extent
313 detectable by the isotope-ratio mass spectrometer (Fig. 4A).

314 The majority of the fractionation between *P. fluorescens* biomass and the substrate was most
315 likely due to discrimination against ^{13}C during cellobiose uptake. If we assume that *P.*
316 *fluorescens* secreted organic compounds at a rate of 10% of the sum of SGR and SRR (El-Mansi
317 and Holms, 1989) and that the bacteria did not discriminate against ^{13}C -containing cellobiose
318 during uptake (and thus assimilated cellobiose possessed a $\delta^{13}\text{C}$ of -24.2‰), isotopic mass
319 balance dictates that the $\delta^{13}\text{C}$ of the C secretion flux (Fig. 5) would have to be +70‰, at
320 minimum, across all temperatures. To our knowledge, such high metabolic discrimination
321 against ^{13}C would be very unusual for biological systems (O’Leary, 1981). An alternative and
322 more likely scenario is therefore that *P. fluorescens* took up less ^{13}C -containing cellobiose than
323 was supplied as substrate, and that discrimination during uptake contributed substantially to *P.*

324 *fluorescens* biomass and respired CO₂ being more ¹³C depleted than the cellobiose supplied.
325 This conclusion holds for all temperatures studied. If we assume for the example 23.5 °C
326 chemostat run at steady-state (Figs. 2, 5) that *P. fluorescens* secreted organic compounds at a rate
327 of 10% of the sum of SGR and SRR, and we further assume that the δ¹³C of secreted compounds
328 was 11.7‰ less negative than that of the biomass (Blair et al., 1985), that is -18.1‰, then the
329 δ¹³C of the cellobiose taken up would have been -31.1‰, which is only a 10‰ difference from
330 the cellobiose provided, and therefore probably a more likely scenario (Fig. 5).

331 Substantial ¹³C depletion of respired CO₂ relative to microbial biomass has not, to our
332 knowledge, been reported in other studies. With the microbial C consumption rate amounting to
333 only 2.8% of the rate of C supply, C availability was high compared to what microbes in their
334 natural environments typically experience (Tempest and Neijssel, 1978; Cole et al., 1988;
335 Hobbie and Hobbie, 2013), potentially promoting enzymatic discrimination. The cellobiose δ¹³C
336 of -24.2 ‰ implies a ¹³C/¹²C ratio of ~1/91. Considering the molecular formula of cellobiose
337 C₁₂H₂₂O₁₁, this means that not more than about one out of eight cellobiose molecules in the
338 supplied substrate included a ¹³C atom. Faster diffusion of the isotopically lighter cellobiose
339 molecules may have contributed to a lower probability of ¹³C-containing cellobiose approaching
340 bacterial membrane uptake sites, and hence, to the differences between δ¹³C of substrate and
341 biomass (Fig. 4A). However, isotope fractionation during diffusion – a physical process
342 dependent on compound mass – would likely exhibit a continuous temperature response. Thus,
343 it seems unlikely that fractionation during diffusion was the primary driver of the pronounced,
344 discontinuous changes in the difference between substrate and biomass δ¹³C, which ranged from
345 5.5 to 10.5‰ (Fig. 4A). Rather, this variation, with one apparently linear part between 13 °C and
346 16 °C and another between 18 °C and 23.5 °C, may be explained parsimoniously by a

347 significant, discontinuous reorganization of enzyme-mediated C fluxes into and out of bacterial
348 cells (see Nanchen et al., 2006), induced by differences in temperature at which *P. fluorescens*
349 was growing and the related differences in substrate uptake rates.

350 Evidence from work on C isotope distribution within carbohydrate molecules (e.g., Rossmann et
351 al., 1991; Gleixner and Schmidt, 1997) suggests non-random distribution of ^{13}C in biological
352 molecules (such as cellobiose). Based on such phenomena, it is probable that the ^{13}C atom in
353 ^{13}C -containing cellobiose was consistently at the same position within the molecule, which rules
354 out the possibility that any changes in the intramolecular ^{13}C distribution of cellobiose were
355 responsible for the observed $\delta^{13}\text{C}$ patterns in biomass and respired CO_2 (Fig. 4). Hence, the
356 discontinuous pattern of $\delta^{13}\text{C}$ of respired CO_2 with temperature, similar to the pattern for $\delta^{13}\text{C}$ of
357 the biomass (Fig. 4A), presumably reflects the downstream consequence of an upstream change
358 in $\delta^{13}\text{C}$ of the metabolic substrate taken up and ultimately respired. However, the more negative
359 $\delta^{13}\text{C}$ of respired CO_2 compared to that of biomass is, to our knowledge, the most direct evidence
360 to date for ^{13}C discrimination during respiration of a heterotrophic microbe. The observation of a
361 substantial respiratory ^{13}C discrimination corroborates inferences drawn in earlier studies
362 (Šantrůčková et al., 2000; Fernandez and Cadisch, 2003) and is also consistent with plant studies
363 reporting C isotope discrimination during dark respiration in roots (Klumpp et al., 2005;
364 Bathellier et al., 2009; Ghashghaie and Badeck, 2014). Our observations of respiratory
365 discrimination against ^{13}C highlight the similarity of heterotrophic, aerobic respiratory pathways,
366 and isotope effects within them, across life's domains.

367 In contrast to the discontinuous relationship between biomass $\delta^{13}\text{C}$ and temperature, we observed
368 a comparably continuous and linear increase in respiratory discrimination against ^{13}C with

369 temperature (Fig. 4B). This increase generated a marginally positive significant ($P=0.08$)
370 correlation with SRR (Fig. 6), and hence a marginally significant ($P=0.07$) correlation with CUE.
371 A physiological interpretation of this finding is not straightforward, as multiple, possibly
372 simultaneous enzymatic fractionations may have contributed to the observed $\delta^{13}\text{C}$ of respired
373 CO_2 (Dijkstra et al., 2011; Tcherkez et al., 2012). It could simply result from a proportionally
374 increasing flux through respiratory pathways, with associated stronger expression of ^{13}C
375 discrimination by the enzymes involved (Tcherkez et al., 2012), or could result from increasing
376 temperatures altering the relative fluxes through respiratory pathways (Chung et al., 1976;
377 Wittmann et al., 2007; Dijkstra et al., 2011) such that the overall observed respiratory ^{13}C
378 discrimination increased with temperature. This may be possible given that respiratory pathways
379 can exhibit distinct fractionation factors (Bathellier et al., 2009 and references therein) and
380 prompt different, specific C atoms to undergo decarboxylation from the two glucose units of the
381 substrate cellobiose, which contain non-randomly distributed ^{13}C atoms (Rossmann et al., 1991;
382 Gleixner and Schmidt, 1997). If relative fluxes through different respiratory pathways changed
383 with temperature, the continuous nature of the relationship between temperature and respiratory
384 ^{13}C discrimination suggests a smooth transition compared to the abrupt and discontinuous shifts
385 in apparent uptake and/or secretion discrimination described above. Future metabolic flux
386 analyses linked to isotopic approaches sensitive enough to quantify C isotopes in microbial
387 exudation will be well-suited to explore how C allocation to distinct, aerobic respiratory
388 pathways may vary with temperature and result in varying $\delta^{13}\text{C}$ of respired CO_2 .

389

390 **4. Conclusions**

391 Our observations clearly show a decline in microbial CUE with increasing temperature when C
392 substrate is plentiful and demonstrate the mechanism driving it – an increase in SRR. The
393 relationship between CUE and temperature underscores the importance of incorporating variable,
394 temperature dependent SRR, which influences CUE and growth efficiency, in ecosystem process
395 models. The temperature-driven changes in SRR and respiratory discrimination against ^{13}C were
396 not independent of each other, suggesting that increasing SRR, to some degree, drives enhanced
397 C isotopic discrimination. We demonstrate that C isotope discrimination associated with
398 microbial decomposition of OM can impart large and variable isotopic signatures on C pools
399 typically characterized and interpreted in biogeochemical studies at any scale. To date, efforts to
400 partition flux components of net ecosystem exchange have assumed little to no fractionation
401 between respired substrates and the resultant CO_2 . Our results suggest that this assumption must
402 be reevaluated, and represent a first step towards an isotopically explicit, mechanistic framework
403 for microbial C isotope fluxes in Earth system models.

404

405 **Author contribution:**

406 C.A.L. and K.M. performed the experiments; all authors contributed to all other parts and stages
407 of the manuscript.

408

409 **Data availability:** The data presented in this study are available for collaborative use by anyone
410 interested; contact the corresponding author for access to the data.

411

412 **Acknowledgements:**

413 We thank Dr. Susan Ziegler, Dr. Jarad Mellard and Chao Song for helpful discussions during the
414 design of the experiments, Greg Caine for expert stable isotope analysis and the provision of
415 isotopic standards, Drs. Susan Ziegler, Mike Burrell, Karl Auerswald, Hanns-Ludwig Schmidt
416 and John Kelly for comments on the manuscript, Gil Ortiz with assistance generating Figure 5,
417 anonymous referees for their time and constructive comments, and the National Science
418 Foundation of the USA for funding (grant no. DEB-0950095 and EAR-1331846).

419

420 **References:**

421 Abraham, W.-R., Hesse, C., and Pelz, O.: Ratios of carbon isotopes in microbial lipids as an
422 indicator of substrate usage, *App. Environ. Microbiol.*, 64, 4202-4209, 1998.

423 Allison, S.D., Wallenstein, M.D., and Bradford, M.A.: Soil-carbon response to warming
424 dependent on microbial physiology, *Nat. Geosci.*, 3, 336-340, 2010.

425 Apple, J.K., del Giorgio, P.A., and Kemp, W.M.: Temperature regulation of bacterial production,
426 respiration, and growth efficiency in a temperate salt-marsh estuary, *Aquat. Microb. Ecol.*, 43,
427 243-254, 2006.

428 Barbosa, I.C.R., Köhler, I.H., Auerswald, K., Lüps, P., and Schnyder, H.: Last-century changes of
429 alpine grassland water-use efficiency: a reconstruction through carbon isotope analysis of a time-
430 series of *Capra ibex* horns, *Glob. Change Biol.*, 16, 1171-1180, 2010.

431 Bathellier, C., Tcherkez, G., Bligny, R., Gout, E., Cornic, G., and Ghashghaie, J.: Metabolic
432 origin of the $\delta^{13}\text{C}$ of respired CO_2 in roots of *Phaseolus vulgaris*, *New Phytol.*, 181, 387-399,
433 2009.

434 Billings, S.: Soil organic matter dynamics and land use change at a grassland/forest ecotone, *Soil*
435 *Biol. Biochem.*, 38, 2934-2943, 2006.

436 Blair, N., Leu, A., Muñoz, E., Olsen, J., Kwong, E., and Des Marais, D.: Carbon isotopic
437 fractionation in heterotrophic microbial metabolism, *Appl. Environ. Microbiol.*, 50, 996-1001,
438 1985.

439 Bowling, D.R., Pataki, D.E., and Randerson, J.T.: Carbon isotopes in terrestrial ecosystem pools
440 and CO_2 fluxes, *New Phytol.*, 178, 24-40, 2008.

441 Brüggemann, N., Gessler, A., Kayler, Z., Keel, S.G., Badeck, F., Barthel, M., Boeckx, P.,
442 Buchmann, N., Brugnoli, E., Esperschütz, J., Gavrichkova, O., Ghashghaie, J., Gomez-
443 Casanovas, N., Keitel, C., Knohl, A., Kuptz, D., Palacio, S., Salmon, Y., Uchida, Y., and Bahn,
444 M.: Carbon allocation and carbon isotope fluxes in the plant-soil-atmosphere continuum: a
445 review, *Biogeosci.*, 8, 3457-3489, 2011.

446 Bull, A.T.: The renaissance of continuous culture in the post-genomics age, *J. Ind. Microbiol.*
447 *Biotechnol.*, 37, 993-1021, 2010.

448 Chrzanowski, T.H., and Grover J.P.: Element content of *Pseudomonas fluorescens* varies with
449 growth rate and temperature: A replicated chemostat study addressing ecological stoichiometry,
450 *Limnol. Oceanogr.*, 53, 1242-1251, 2008.

451 Chung, B.H., Cannon, R.Y., and Smith, R.C.: Influence of growth temperature on glucose
452 metabolism of a psychrotrophic strain of *Bacillus cereus*, *Appl. Environ. Microb.*, 31, 39-45,
453 1976.

454 Cleland, W.W.: The use of isotope effects to determine enzyme mechanisms, *Arch. Biochem.*
455 *Biophys.*, 433, 2-12, 2005.

456 Cole, J.J., Findlay, S., and Pace M.L.: Bacterial production in fresh and saltwater ecosystems: a
457 cross-system overview, *Mar. Ecol. Prog. Ser.*, 43, 1-10, 1988.

458 Cotner, J.B., and Biddanda, B.A.: Small players, large role: microbial influence on
459 biogeochemical processes in pelagic aquatic ecosystems, *Ecosystems*, 5, 105-121, 2002.

460 Cotner, J.B., Makino, W., and Biddanda, B.A.: Temperature affects stoichiometry and
461 biochemical composition of *Escherichia coli*, *Microb. Ecol.*, 52, 26-33, 2006.

462 Craig, H., and Gordon, L.I.: Deuterium and ^{18}O oxygen variations in the ocean and the marine
463 atmosphere. In: *Proceedings of a conference on stable isotopes in oceanographic studies and*
464 *paleotemperatures*. Ed: E. Tongiori, Lischi & Figli, Pisa, 1965.

465 Dawson, P.S.S.: *Microbial growth*, Dowden, Hutchinson & Ross, Stroudsburg, 1974.

466 del Giorgio, P.A., and Cole, J.J.: Bacterial growth efficiency in natural aquatic systems, *Annu.*
467 *Rev. Ecol. Syst.*, 29, 503-541, 1998.

468 Dijkstra, F.A., Hobbie, S.E., Knops, J.M.H., and Reich, P.B.: Nitrogen stabilization and plant
469 species interact to influence soil carbon stabilization, *Ecol. Lett.*, 7, 1192-1198, 2004.

470 Dijkstra, P., Thomas, S.C., Heinrich, P.L., Koch, G.W., Schwartz, E., and Hungate, B.A.: Effect
471 of temperature on metabolic activity of intact microbial communities: evidence for altered
472 metabolic pathway activity but not for increased maintenance respiration and reduced carbon use
473 efficiency, *Soil Biol. Biochem.*, 43, 2023-2031, 2011.

474 Egli, T.: Microbial growth and physiology: a call for better craftsmanship, *Front. Microbiol.*,
475 6:287, DOI: 10.3389/fmicb.2015.00287, 2015.

476 El-Mansi, E.M.T., Holms, W.H.: Control of carbon flux to acetate excretion during growth of
477 *Escherichia coli* in batch and continuous cultures, *J. General Microbiol.*, 135, 2875-883, 1989.

478 Farquhar, G.D., O'Leary, M.H., and Berry, J.A.: On the relationship between carbon isotope
479 discrimination and the intercellular carbon dioxide concentration in leaves, *Aust. J. Plant
480 Physiol.*, 9, 121-137, 1982.

481 Farquhar, G.D., and Richards, R.A.: Isotopic composition of plant carbon correlates with water-
482 use efficiency of wheat genotypes, *Aust. J. Plant Physiol.*, 11, 539-552, 1984.

483 Ferenci, T.: Bacterial physiology, regulation and mutational adaptation in a chemostat
484 environment, *Adv. Microb. Physiol.*, 53, 169-230, 2008.

485 Fernandez, I., and Cadisch, G.: Discrimination against ^{13}C during degradation of simple and
486 complex substrates by two white rot fungi, *Rapid Commun. Mass Spectrom.*, 17, 2614-2620,
487 2003.

488 Frey, S., Lee, J., Melillo, J.M., and Six, J.: The temperature response of soil microbial efficiency
489 and its feedback to climate, *Nat. Clim. Change*, 3, 395-398, 2013.

490 Fry, B.: *Stable Isotope Ecology*, Springer, New York, 2006.

491 Gamnitzer, U., Moyes, A.B., Bowling, D.R., and Schnyder, H.: Measuring and modeling the
492 isotopic composition of soil respiration: insights from a grassland tracer experiment, *Biogeosci.*,
493 8, 333-1350, 2011.

494 Ghashghaie, J., and Badeck, F.W.: Opposite carbon isotope discrimination during dark
495 respiration in leaves versus roots – a review, *New Phytol.*, 201, 751-769.

496 Gillooly, J.F., Brown, J.H., West, G.B., Savage, V.M., and Charnov, E.L.: Effects of size and
497 temperature on metabolic rate, *Science*, 293, 2248-2251, 2001.

498 Gleixner, G., and Schmidt H.-L.: Carbon isotope effects on the Fructose-1,6-bisphosphate
499 aldolase reaction, origin for non-statistical ^{13}C distributions in carbohydrates, *J. Biol. Chem.*,
500 272, 5382-5387, 1997.

501 Goldman, J.C., and Dennet, M.R.: Growth of marine bacteria in batch and continuous culture
502 under carbon and nitrogen limitation, *Limnol. Oceanogr.*, 45, 789-800, 2000.

503 Hall, E.K., Neuhauser, C., and Cotner, J.B.: Toward a mechanistic understanding of how natural
504 bacterial communities respond to changes in temperature in aquatic ecosystems. *ISME J.*, 2, 471-
505 481, 2008.

506 Hanson, P.J., Edwards, N.T., Garten, C.T., and Andrews, J.A.: Separating root and microbial
507 contributions to soil respiration: a review of methods and observations. *Biogeochem.*, 48, 115-
508 146, 2000.

509 Hedges, J.I., Eglinton, G., Hatcher, P.G., Kirchman, D.L., Arnosti, C., Derenne, S., Evershed,
510 R.P., Kögel-Knabner, I., de Leeuw, J.W., Littke, R., Michaelis, W., Rullkötter, J.: The
511 molecularly-uncharacterized component of nonliving organic matter in natural environments,
512 *Org. Geochem.*, 31, 945-958, 2000.

513 Hobbie, J.E., and Hobbie, E.A.: Microbes in nature are limited by carbon and energy: the
514 starving-survival lifestyle in soil and consequences for estimating microbial rates, *Front.*
515 *Microbiol.*, 4, doi: 10.3389/fmicb.2013.00324, 2013.

516 Kayser, A., Weber, J., Hecht, V., and Rinas, U.: Metabolic flux analysis of *Escherichia coli* in
517 glucose-limited continuous culture. I. Growth-rate dependent metabolic efficiency at steady-
518 state, *Microbiol.*, 151, 693-706, 2005.

519 Kirschbaum, M.U.F.: The temperature-dependence of organic-matter decomposition – still a
520 topic of debate, *Soil Biol. Biochem.*, 38, 2510-2518, 2006.

521 Klumpp, K., Schäufele, R., Lötscher, M., Lattanzi, F.A., Feneis, W., and Schnyder, H.: C-isotope
522 composition of CO₂ respired by shoots and roots: fractionation during dark respiration?, *Plant*
523 *Cell Environ.*, 28, 241-250, 2005.

524 Kucera, C.L., and Kirkham, D.R.: Soil respiration studies in tallgrass prairie in Missouri,
525 *Ecology*, 52, 912-915, 1971.

526 Lehmeier, C.A., Min, K., Niehues, N.D., Ballantyne, F.IV., and Billings, S.A.: Temperature-
527 mediated changes of exoenzyme-substrate reaction rates and their consequences for the carbon to
528 nitrogen flow ration of liberated resources, *Soil Biol. Biochem.*, 57, 374-382, 2013.

529 Manzoni, S., Taylor, P., Richter, A., Porporato, A., and Ågren, G.I.: Environmental and
530 stoichiometric controls on microbial carbon-use efficiency in soils, *New Phytol.*, 196, 79-91,
531 2012.

532 Min, K., Lehmeier, C.A., Ballantyne, F., Tatarko, A., and Billings, S.A.: Differential effects of
533 pH on temperature sensitivity of organic carbon and nitrogen decay, *Soil Biol. Biochem.*, 76,
534 193-200, 2014.

535 Mook, W.G., Bommerson, J.C., and Staverman, W.H.: Carbon isotope fractionation between
536 dissolved bicarbonate and gaseous carbon dioxide, *Earth Planet. Sci. Lett.*, 22, 169-176, 1974.

537 Nanchen, A., Schicker A., and Sauer U.: Nonlinear dependency of intracellular fluxes on growth
538 rate in miniaturized continuous cultures of *Escherichia coli*, *Appl. Environ. Microb.*, 73, 1164-
539 1172, 2006.

540 Nickerson, N., Egan, J., and Risk, D.: Iso-FD: A novel method for measuring the isotopic
541 signature of surface flux, *Soil Biol. Biochem.*, 62, 99-106, 2013.

542 O'Leary, M.H.: Carbon isotope fractionation in plants, *Phytochem.*, 20, 553-567, 1981.

543 Park, R., and Epstein, S.: Metabolic fractionation of C¹³ & C¹² in plants, *Plant Physiol.*, 36, 133-
544 138, 1961.

545 Pataki, D.E., Ehleringer, J.E., Flanagan, L.B., Yakir, D., Bowling, D.R., Still, C.J., Buchmann,
546 N., Kaplan, J.O., and Berry, J.A.: The application and interpretation of Keeling plots in terrestrial
547 carbon cycle research, *Glob. Biogeochem. Cycles*, 17, doi:10.1029/2001GB001850, 2003.

548 Pomeroy, L.R., and Wiebe, W.J.: Temperature and substrate as interactive limiting factors for
549 marine heterotrophic bacteria, *Aquat. Microb. Ecol.*, 23, 187-204, 2001.

550 Rivkin, R.B., and Legendre, L.: Biogenic carbon cycling in the upper ocean: effects of microbial
551 respiration, *Science*, 291, 2398-2400, 2001.

552 Rossmann, A., Butzenlechner, M., and Schmidt, H.L.: Evidence for a nonstatistical carbon
553 isotope distribution in natural glucose, *Plant Physiol.*, 96, 609-614, 1991.

554 Šantrůčková, H., Bird, M.I., and Lloyd, J.: Microbial processes and carbon-isotope fractionation
555 in tropical and temperate grassland soils, *Funct. Ecol.*, 14, 108-114, 2000.

556 Schimel, D.S.: Terrestrial ecosystems and the carbon-cycle, *Glob. Change Biol.*, 1, 77-91, 1995.

557 Smith, H.L., and Waltman, P.E.: The theory of the chemostat: dynamics of microbial
558 competition, Cambridge University Press, New York, 1995.

559 Stumm, W., and Morgan, J.J.: Aquatic Chemistry: An introduction emphasizing chemical
560 equilibria in natural waters, John Wiley & Sons, New York, 1981.

561 Subke, J.-A., Inglima, I., and Cotrufo, M.F.: Trends and methodological impacts in soil CO₂ flux
562 partitioning: A metaanalytical review, *Glob. Change Biol.*, 12, 921-943, 2006.

563 Szaran, J.: Achievement of carbon isotope equilibrium in the system HCO₃⁻ (solution) – CO₂
564 (gas). *Chem. Geol.*, 142, 79-86, 1997.

565 Tcherkez, G., Mahé, A., and Hodges, M.: ¹²C/¹³C fractionations in plant primary metabolism,
566 Trends Plant Sci., 16, 499-506, 2012.

567 Tempest, D.W., and Neijssel, O.M.: Eco-physiological aspects of microbial growth in aerobic
568 nutrient-limited environments, *Adv. Microb. Ecol.*, 2, 105-153, 1978.

569 Trumbore, S.: Carbon resired by terrestrial ecosystems – recent progress and challenges, *Glob.*
570 *Change Biol.*, 12, 141-153, 2006.

571 Tucker, C.L., Bell, J., Pendall, E., and Ogle, K.: Does declining carbon-use efficiency explain
572 thermal acclimation of soil respiration with warming?, *Glob. Change Biol.*, 19, 252-263, 2013.

573 Vogel, J.C., Grootes, P.M., and Mook, W.G.: Isotopic fractionation between gaseous and
574 dissolved carbon dioxide, *Z. Physik*, 230, 225-238, 1970.

575 Werner, C., and Gessler, A.: Diel variations in the carbon isotope composition of respired CO₂
576 and associated carbon sources: a review of dynamics and mechanisms, *Biogeosci.*, 8, 2437-2459,
577 2011.

578 Werner, R.A., Buchmann, N., Siegwolf, R.T.W., Kornexl, B.E., and Gessler, A.: Metabolic
579 fluxes, carbon isotope fractionation and respiration – lessons to be learned from plant
580 biochemistry, *New Phytol.*, 191, 10-15, 2011.

581 Werth, M., and Kuzyakov, Y.: ¹³C fractionation at the root-microorganisms-soil interface: a
582 review and outlook for partitioning studies, *Soil Biol. Biochem.*, 42, 1372-1384, 2010.

583 Wieder, W.R., Bonan, G.B., and Allison, S.D.: Global soil carbon projections are improved by
584 modelling microbial processes, *Nat. Clim. Change*, 3, 909-912, 2013.

585 Wittmann, C., Weber, J., Betiku, E., Krömer, J., Böhm, D., and Rinas, U.: Response of fluxome
586 and metabolome to temperature-induced recombinant protein synthesis in *Escherichia coli*, J.
587 Biotechnol., 132, 375-384, 2007.

588

589

590

591

592

593

594

595

596

597

598

599

600

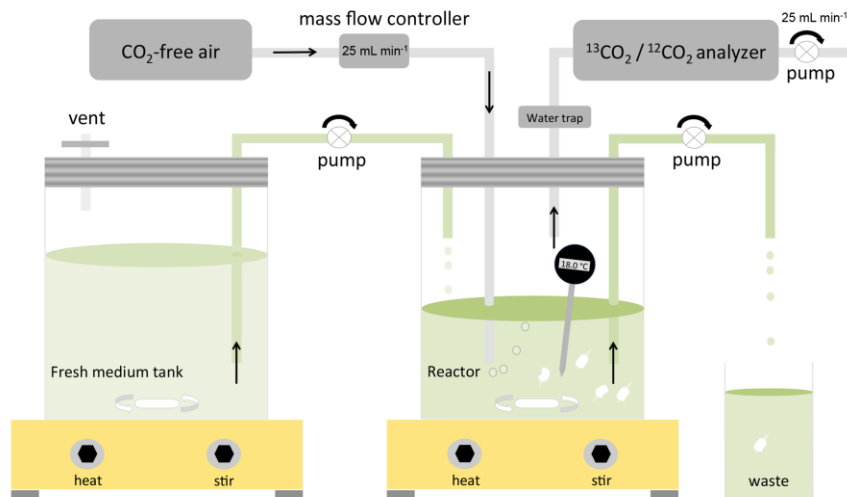
601

602

603 **Figures:**

604 **Fig. 1.** Chemostat system comprised of *P. fluorescens* growing on cellobiose. Seven independent
605 experiments were conducted, with reactor temperatures of 13, 14.5, 16, 18, 21, 23.5 and 26.5 °C;
606 all other conditions were identical. During continuous flow, dilution rate of the reactor
607 (mean=0.137±0.01 h⁻¹ across all experiments) equals microbial growth rate. A peristaltic pump
608 supplied fresh nutrient medium from a reservoir tank to the reactor and removed reactor medium
609 (including biomass) at a constant rate. Headspace volume was flushed with CO₂-free air,
610 bubbling through reactor medium and supplying microorganisms with O₂. A ¹³CO₂/¹²CO₂
611 analyzer continuously sampled reactor headspace and measured the concentration and δ¹³C of
612 respired CO₂.

613

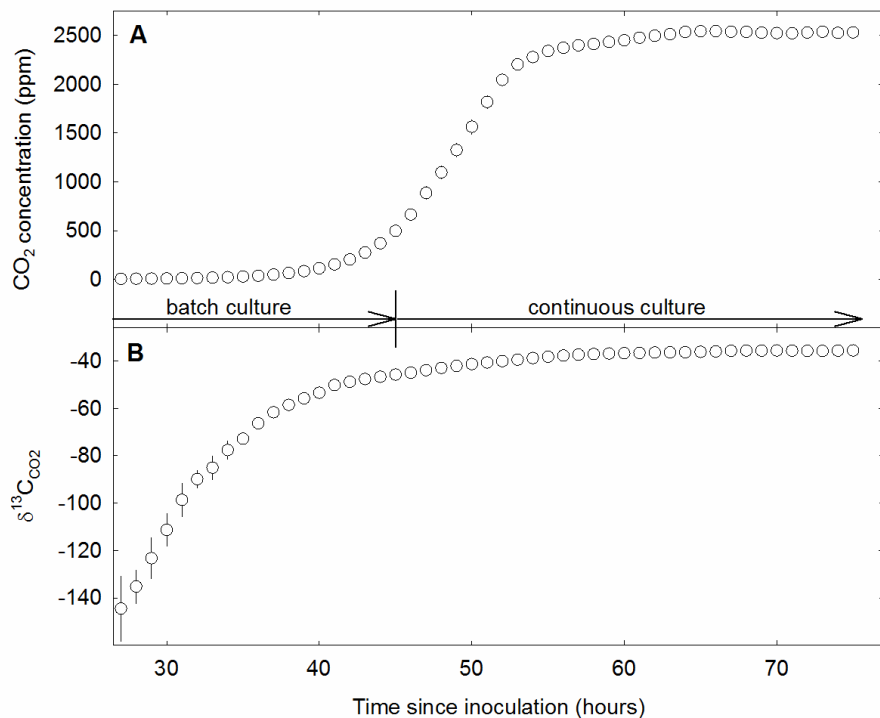


614

615

616 **Fig. 2.** Example time course of the evolution of reactor headspace CO_2 concentration (A) and
617 $\delta^{13}\text{C}$ of the CO_2 (B) of the chemostat run at 23.5 °C in hours since inoculation of the reactor with
618 pre-cultured *P. fluorescens*. Data points are hourly means. Error bars (where visible) denote ± 1
619 SD. The reactor was shifted from batch to continuous culture mode 45 h after inoculation.
620 Microbial respiration rate and the $\delta^{13}\text{C}$ of respired CO_2 were measured between 70 and 74 h after
621 inoculation when the culture reached steady-state.

622

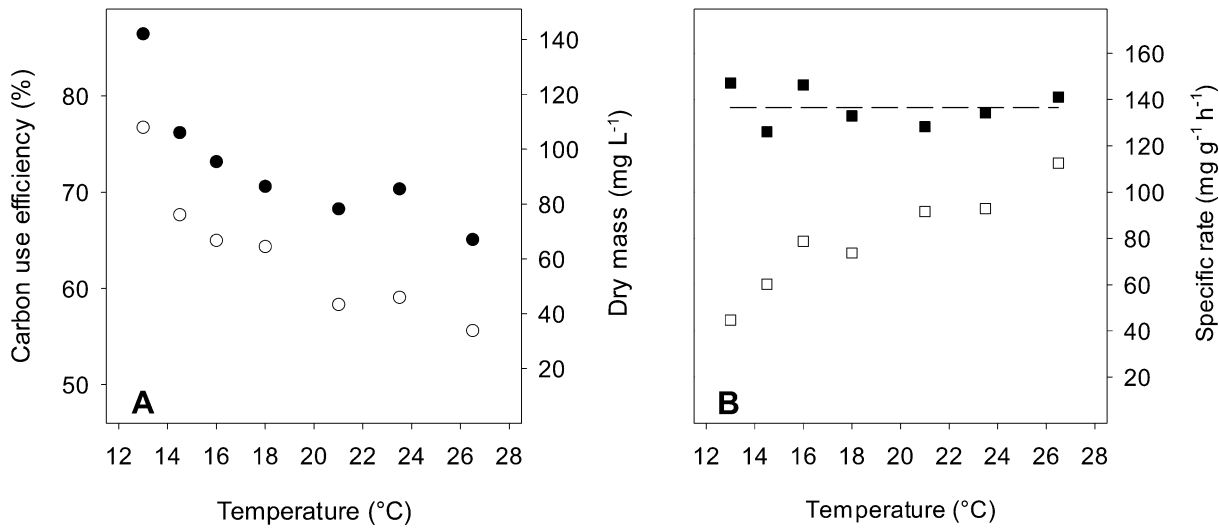


623

624

625 **Fig. 3.** Steady-state process variables of *P. fluorescens* growing in chemostats at specified
626 temperatures. Microbial carbon use efficiency (○; A), dry microbial biomass (●; A), specific C
627 growth rate (■; B), and specific C respiration rate (□; B), expressed per unit of microbial
628 biomass-C. The dashed line denotes the average of the seven specific growth rates (137 mg g⁻¹
629 h⁻¹).

630



631

632

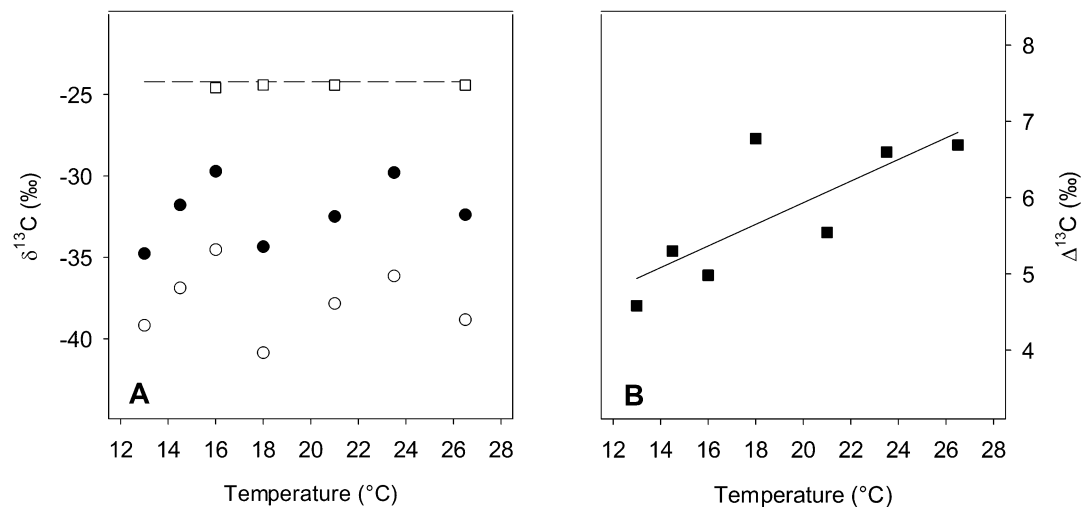
633

634

635

636 **Fig. 4.** Steady-state $\delta^{13}\text{C}$ of microbial biomass (●; A) and of respired CO_2 (○; A), and C isotope
 637 discrimination during respiration ($\Delta^{13}\text{C}$; B) of *P. fluorescens* growing in chemostats at specified
 638 temperatures. In panel A, the dashed line denotes the $\delta^{13}\text{C}$ of the substrate cellobiose (-24.2‰),
 639 and $\delta^{13}\text{C}$ of reactor filtrate is shown as open squares; standard errors, derived from multiple
 640 measurements across time during steady-state, are smaller than the size of the symbols. $\Delta^{13}\text{C}$ is
 641 calculated as $\Delta^{13}\text{C} = (\delta^{13}\text{C}_{\text{biomass}} - \delta^{13}\text{C}_{\text{respired CO}_2}) / (1 + \delta^{13}\text{C}_{\text{respired CO}_2})$. The solid line denotes
 642 linear regression of $\Delta^{13}\text{C}$ vs. temperature ($y = 0.14x + 3.1$; $R^2 = 0.61$; $P=0.04$).

643



644

645

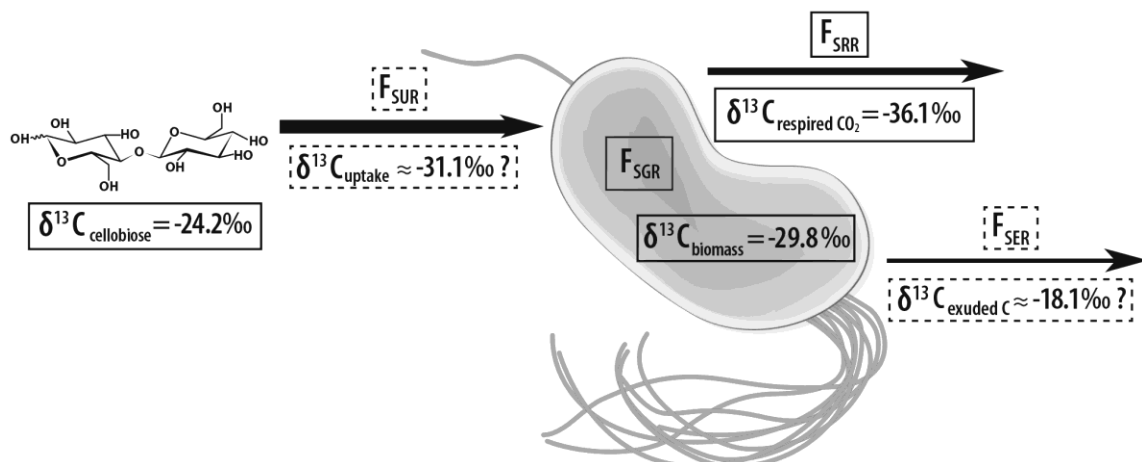
646

647

648 **Fig. 5.** Schematic of an individual *P. fluorescens* cell, representing the sample population
 649 growing at 23.5 °C with one available substrate at a constant relative growth rate of 0.13 h⁻¹ at
 650 steady-state (Fig. 2), with measured (solid boxed) and estimated (dashed boxed) magnitudes of C
 651 and ¹³C fluxes into and out of the population. Designated fluxes include specific uptake rate of
 652 cellobiose (F_{SUR}), specific growth rate (F_{SGR}), specific respiration rate (F_{SRR}) and specific
 653 excretion rate (F_{SER}), in relation to steady-state biomass-C in the chemostat, where $F_{SUR} = F_{SGR} +$
 654 $F_{SRR} + F_{SER}$. The estimate of $\delta^{13}\text{C}_{\text{uptake}}$ is based on the assumption that $\delta^{13}\text{C}_{\text{exuded C}}$ is 11.7‰ less
 655 negative than $\delta^{13}\text{C}_{\text{biomass}}$ (Blair et al., 1985) and that F_{SER} is 10% of the sum of F_{SGR} and F_{SRR} (El-
 656 Mansi and Holms, 1989). In contrast to this experimental system, in natural environments
 657 measurements of boxed pools and fluxes can be confounded by the presence of dormant
 658 microorganisms, unknown microbial growth rates, diverse available substrates, and a lack of
 659 steady-state CO₂ fluxes.

660

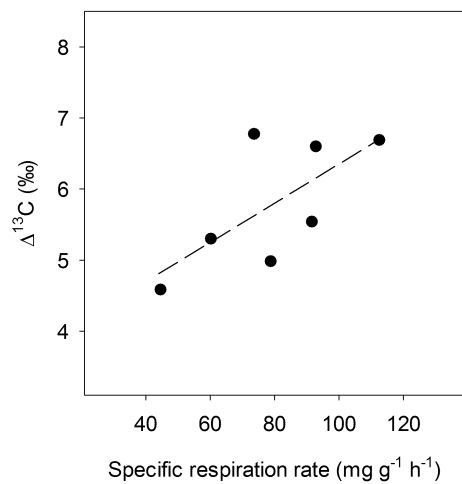
661



662

663 **Fig. 6.** Correlation between the specific respiration rate of *P. fluorescens* growing in continuous
664 chemostat culture at temperatures ranging from 13 °C to 26.5 °C and the carbon isotope
665 discrimination during respiration. The dashed line denotes a linear regression of the form $y =$
666 $0.03x + 3.6$; $R^2 = 0.48$; $P = 0.08$.

667



668